Experimental studies of packed-bed Thermal Energy Storage system performance

Jakub Ochmann[1][*][✉], Łukasz Bartela[1], Krzysztof Rusin[1], Michał Jurczyk[1], Bartosz Stanek[1], Sebastian Rulik[1], Sebastian Waniczek[2],

[1]Silesian University of Technology, Faculty of Energy and Environment Engineering, Department of Power Engineering and Turbomachinery, 18 Konarskiego street, 44-100 Gliwice, Poland
[✉] jakub.ochmann@polsl.pl
[2]Energoprojekt-Katowice S.A., 15 Jesionowa street, 40-159 Katowice, Poland

Abstract

This paper contains an experimental analysis of a heat storage tank's heat loss and exergy efficiency using a basalt porous bed as a storage material. The basic parameters of the laboratory bench with measuring equipment are presented and the experimental procedure is discussed. The methodology for evaluating the energy potential of the heat storage process for large-scale energy storage systems is described. The main novelty of the presented system is the application of the slenderness of the heat accumulator, which corresponds to the development of the system in a post-mining shaft. Based on the analysis of the experiment, the exergy cycle efficiency of the heat storage unit was determined to equal 52.3%, and the energy efficiency equal to 96.6%.

Keywords: thermal energy storage (TES), exergy, packed bed, adiabatic compressed air energy storage system (A-CAES),

Introduction

Changing trends in the conventional energy sector and the rise of decentralized power generation are increasing the demand for large-scale energy storage systems [1]. These changes also affect local socio-economic development due to the region's dependence on heavy industry and the extraction of natural underground resources [2]. Systems that directly link renewable energy sources and compensate for fluctuations in demand and grid power generation include the power to gas (P2G) [3] or power to gas to power (P2G2P) systems that propose hydrogen or synthetic natural gas (SNG) [4] as an energy carrier. Successful decarbonization of mining-oriented countries and the use of fossil resources could also be possible by proposing and implementing methods to revitalize post-mining areas [5]. One proposed solution is an adiabatic compressed gas energy storage system. This type of system provides for the installation of a compressed gas reservoir and a Thermal Energy Storage tank in the volume of a post-mining shaft [6]. The heat generated during gas compression is stored in a TES reservoir, whose accumulating material can be single-phase [7] and phase change materials [8]. During system discharge, the heat is transferred to the expanded gas, which is directed to the expander [9]. Experimental and numerical studies of heat storage operation will evaluate the feasibility of using porous deposits as heat storage within adiabatic energy storage systems [10]. The exergy efficiency of the storage operation cycle is proposed to verify the usability of the system, as an assessment of not only the quantitative performance of heat transfer and storage but also the qualitative functionality considering the energy dispersion within the rock material [11]. The main challenge in installing the system in post-mining infrastructure is to develop solutions to guarantee the integrity of the mine shaft casing [12]. Experimental studies are essential in modeling large-scale energy storage systems, which are made possible by applying numerical fluid mechanics to mass and heat flow calculations [13]. Experimental data provide the basis for validation of numerical models, where the primary searches are the heat transfer intensity between the medium and the pressure drop of the flowing medium [14].

Laboratory stand configuration

The laboratory-scale Thermal Energy Storage was located in the Department of Power Engineering and Turbomachinery at the Silesian University of Technology. The main component of the stand is a vertical tank with a 3 meters height and a diameter of DN219. The filling of the tank, and thus the heat

storage material, is basalt grit with an average diameter of 15.5 mm. The total volume of the rock material is 0.1 m³ and the mass is 174 kg. Calculations indicated that the average porosity of the rock deposit is about 0.38 with an increase in this value in the radial direction near the tank wall [15]. The flow medium is low-pressure air, which is pumped into the system by a 7.5 kW side channel blower that could produce up to 39.5 kPa. The air is heated by a 17 kW Lester model LE 10000 electric heater. The control system allows for determining the maximum temperature of the air supplying the storage tank. The TES tank with its labeled temperature measurement points is shown in Figure 1.
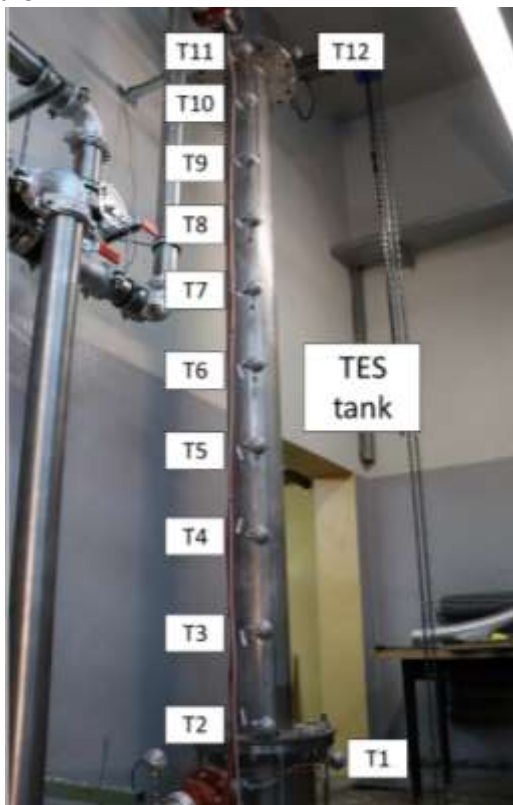
Figure 1: Laboratory-scale Thermal Energy Storage tank

The basalt temperature is measured in real-time using ten resistive temperature detectors (T11 - T2) with an accuracy of ±0.15 K equally spaced from each other along the tank axis. In addition, the inlet and outlet air from the heat storage tank (T1 and T12) is also measured. Control of the blower power and consequently the airflow through the system is carried out by a static frequency converter. An increase in fan power increases motor temperature, which directly affects the temperature of the air supplied to the system. The characteristic of the supply air temperature as a function of the mass flow rate of this air is shown in Figure 2.
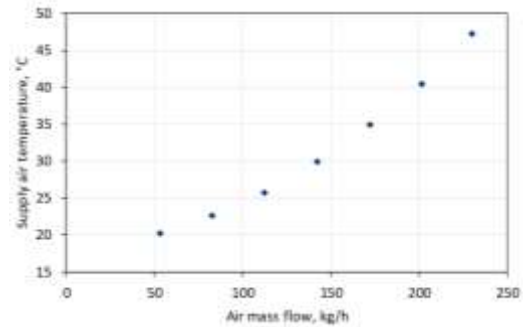
Figure 2: Dependence of air temperature on mass flow rate

The increase in the value of air mass flux also affects the velocity of airflow through the stone bed, and consequently the value of air pressure drop. The value of air pressure drop is measured via a differential pressure transducer with a range of 10 kPa. The laboratory stand is also equipped with a measuring orifice with an accuracy of 0.736%, which allows the measurement of the velocity of airflow through an installation with a diameter of DN90. Knowing the average porosity of the rock bed, the dependence of the velocity of airflow through the volume of the heat storage tank on the mass flux of air was determined.
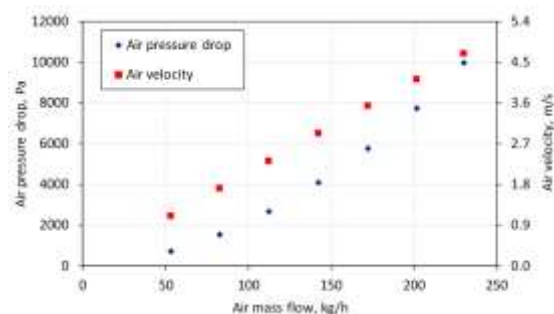
Figure 3: Dependence of air pressure drop and air velocity in packed bed on mass flow rate

A proportional relationship between the airflow velocity in the porous bed on the mass flow rate was demonstrated. For an air mass flow rate of 230 kg/h, the maximum air pressure drop recorded by the differential pressure transducer was achieved.

In addition, ambient temperature and relative humidity are measured at a distance during the operation of the heat storage tank, which excludes the influence of the experiment on the measurement conditions.

Experiment and calculation algorithm

One of the milestones on the way to describing the phenomenon of heating of the storage material and the energy accumulation process is to determine the heat loss to the environment through the side surfaces of the storage tank and to develop a solution to minimize it by using volume-limited thermal insulation to reduce energy dissipation. The degree of heat loss to the environment can be determined dynamically during the operation of the tank based on the tank's external wall temperature data [16] and a calculation of the convective heat transfer coefficient, whose value is also variable over time [17]. The maximum loss to ambient can be determined at the point when the system reaches a steady-state during the charging phase of the heat storage tank. Steady-state is defined as the moment when the basalt temperature rise disappears at all measurement points despite the ongoing flow of hot air through the storage volume. Using the equation for the energy balance of the system:

$$H_{in} = H_{out} + \Delta U_b + Q_{loss} \qquad (1)$$

where H_{in} is the energy of inlet air, H_{out} is the energy of outlet air, ΔU_b is the change of packed bed internal energy and Q_{loss} is the heat loss to the environment.

The measurement procedure for determining the maximum energy loss to ambient was as follows:

- Verification and determination of proper airflow through the heat accumulator.
- Determination of constant side channel blower power.
- Determination by the regulator of the maximum supply air temperature for the heat storage tank.
- Collecting measurement data until the temperature rise of the basalt ceases at the measuring points (T11 - T2).

The enthalpy and energy of the inlet and outlet air were determined from temperature and pressure data using Coolprop software [18]. The effect of moisture on the enthalpy value of the inlet and outlet air was considered in the calculation procedure. The effect of moisture adsorption and desorption on the rock material surface in the heat storage volume was neglected in the calculation. Thus, the relative humidity of the circulating air was estimated from its measured temperature and pressure.

The effectiveness of the TES storage tank interfacing with the CAES is also affected by the quality of energy recovered during the discharge phase. During the heat exchange between two mediums (in the case under consideration, air, and basalt), a temperature difference is observed between the maximum temperature of the hot medium and the maximum achievable temperature of the heated medium. During the heat storage phase, energy is spontaneously dissipated due to temperature differences in the rock bed, leading to a reduction in the maximum energy potential of the stored heat, even though no energy is lost to the environment in a perfectly insulated reservoir. Energy dissipation during the storage phase occurs in two different paths - through heat conduction in the rock material, which is influenced by the thermophysical parameters of the material, and the heat conduction field determined by the tank diameter, and by heat exchange between air and rock material through natural convection within the storage tank. During the discharge phase, there is an analogous phenomenon of the temperature difference between the hot medium (basalt) and the heated medium (air). In addition, there is a drop in air pressure during the charging and discharging phases of the system, which affects the overall performance of the CAES system and the devices interfacing with the TES storage tank ([12], [19]).

The exergy efficiency η_{ex} of a heat storage tank, considering both the quantity and quality of the energy received, was defined as:

$$\eta_{ex} = \frac{Ex_{out}}{Ex_{in}} \qquad (2)$$

where Ex_{out} is the exergy of outlet air and Ex_{in} is the exergy of inlet air.

Exergy of inlet air Ex_{in} was determined as:

$$Ex_{in} = \dot{m}_p \cdot \left[\left(\int_{t=0}^{t=end} h_{in\_c} - \int_{t=0}^{t=end} h_{out\_c} \right) - T_{ot} \cdot \left(\int_{t=0}^{t=end} s_{in\_c} - \int_{t=0}^{t=end} s_{out\_c} \right) \right] \qquad (3)$$

where m_p is the mass flow of air, h_{in_c}, and h_{out_c} are respectively enthalpy of inlet and outlet air during the

charging phase, T_{ot} is the ambient temperature, s_{in_c}, and s_{out_c} are respectively entropy of inlet and outlet air during the charging phase.

$$Ex_{out} = \dot{m}_p \cdot \left[\left[\int_{t=o}^{t=end} h_{in\_d} - \int_{t=0}^{t=end} h_{out\_d} \right. \right. \\ - T_{ot} \\ \left. \left. \cdot \left(\int_{t=0}^{t=end} s_{in\_d} \right. \right. \\ \left. \left. - \int_{t=0}^{t=end} s_{out\_d} \right) \right] \quad (4)$$

where h_{in_d} and h_{out_d} are respectively enthalpy of inlet and outlet air during the discharging phase and s_{in_d} and s_{out_d} are entropy of inlet and outlet air during discharging phase.

Because of the relatively significant height of the heat storage tank, there is a natural temperature gradient of the rock material due to the convective movement of ambient air in the interior. Therefore, to investigate the quality of the stored energy, it is necessary to perform a preheating and cooling process of the bed to equalize the temperature inside the heat storage to the maximum possible extent. Due to the heating of the air caused by the operation of the fan, it is not possible to achieve a discharge air temperature equal to the ambient temperature (Figure 2.). Therefore, it was assumed that the expected initial temperature of the bed is about 30°C, which is equal to the possible temperature of the discharging air. The experimental procedure to investigate the exergy efficiency of the heat storage charging and discharging process was as follows:

- Verification and determination of proper airflow through the heat accumulator.
- Determination of constant side channel blower power.
- Establishing an initial inlet air temperature to limit the temperature gradient of the rock material.
- Determination of the appropriate maximum supply air temperature for the heat storage tank and the start of the charging phase. Initiate recording of measurement data of basalt temperature, air pressure drop, and air mass flux.
- End of the charging phase at the time when no rise in outlet air temperature occurred. The motivation for this procedure was to

avoid a temperature rise in the outlet part of the piping system.
- Disabling the air temperature regulator and stopping the air heating process. Reversing the airflow through the heat storage tank using air dampers.

Results

Maximum heat loss to the environment was calculated under the conditions shown in Table 1.

Table 1: Energy loss calculations - experiment conditions

Variable name	Unit	Value
Average air mass flow	kg/h	199.58
Maximum inlet air temperature	°C	65.5
Average ambient temperature	°C	20.6
Average ambient air humidity	%	41.4

The data presented in Table 1 indicate that the determined air mass flux was a value of approximately 87% of the maximum possible flux. Figure 4 presents data on the increase in basalt temperature at each measurement point during the charging phase of the heat storage tank.
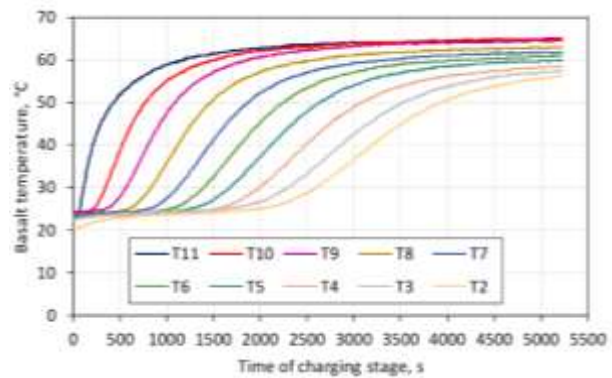
Figure 4: Temperature rise of basalt during the charging stage

The most intense temperature rise was recorded for point T11, which corresponds to the closest point measured to the inlet in the basalt bed. The intensity of temperature rise at this point was equal to 3.5 K/min in the time interval of 0 – 500 s, which corresponds to the period of the most intense

temperature rise. The intensity of the temperature increase of the rock material decreased with each successive measurement point up to point T2, which was closest to the outlet of the reservoir. For this point in the 2500 - 4500 s time range of the charging phase, the intensity of basalt temperature rise was approximately 0.74 K/min. Figure 5 shows the value of air pressure drop and the temperature of the inlet and outlet air from the heat storage tank during the charging phase.
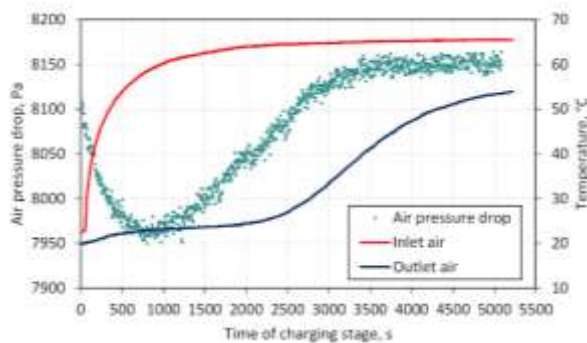
Figure 5: Pressure drop of air and its inlet and outlet temperature during the charging phase

The supply air temperature of the heat storage tank reaches the expected value (Table 1) after approximately 2000 seconds of the charging process. This delay is a result of the loss of energy spent on raising the temperature of the piping system delivering air to the storage tank. At approximately the same time, the outlet air temperature from the heat storage tank increases. This indicates that the air flowing through the heat reservoir is not able to transfer the energy potential to the rock material due to its too high temperature and insufficiently high value of the heat transfer coefficient. The value of air pressure drop increases in the range of 1000 - 3500 s despite no modification in the value of air mass flow rate. This phenomenon results, referring to Ergun's equation [20], from an increase in the temperature of the air in the heat reservoir, which reduces its density while causing an increase in its velocity through the volume of packed-bed material. The difference between the pressure drop value for a cold TES tank is about 200 Pa compared to a hot TES tank. The heat loss to ambient through the walls of the storage tank equaled 645.1 W when the tank reached a steady state. This value was approximately 14% of the energy supplied to the storage tank at the same time. The corresponding

calculation for dry air indicated that the value of heat loss to ambient equaled 636.8 W, indicating a marginal difference between the energy loss values for humid and dry air.

The experiment used to investigate the exergy efficiency of the airflow cycle through the heat storage tank was carried out according to the parameters shown in Table 2.

Table 2: Exergy efficiency calculations - experiment conditions

Variable name	Unit	Value
Average air mass flow	kg/h	130.6
Maximum inlet air temperature	°C	57.5
Average ambient temperature	°C	19.6
Average ambient air humidity	%	26.4

The air mass flux used was only about 57% of the highest possible flux corresponding to the ranges of the measurement devices used. This procedure ensured that the duration of the charging phase was extended without obtaining an increase in the temperature of the air outlet from the reservoir, which would have caused a simultaneous increase in the temperature of the piping system and consequently disrupted the experiment.
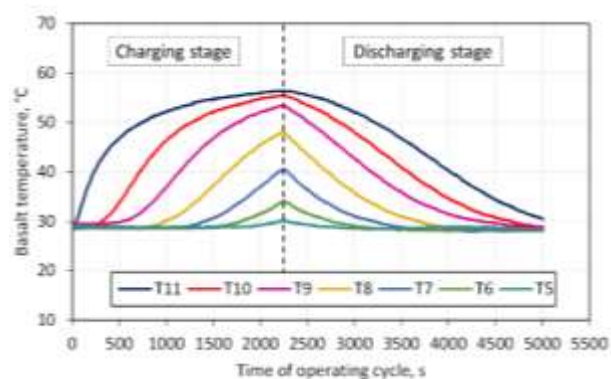
Figure 6: Temperature rise of basalt during the charging and discharging stage

According to the experimental procedure, the initial temperature gradient of the rock material was reduced to a minimum and its temperature was approximately 30°C. The heat storage charging phase

was completed after approximately 2250 seconds of duration and resulted in a slight increase in basalt temperature at the T5 sensor height, which is over half of the heat storage length. At the same time, there was no increase in outlet air temperature. The time required to completely discharge the heat storage tank was longer than the charging phase. This is due to insufficient heat transfer time between the rock material and the air. Figure 7 shows the value of air pressure drop during the heat storage cycle.
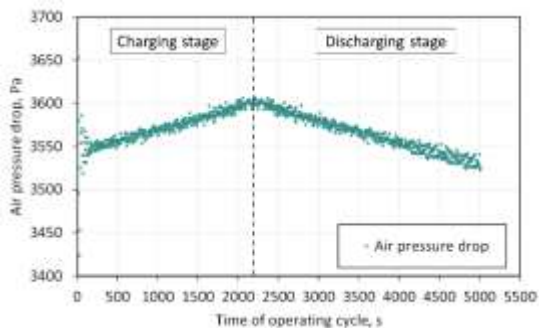
Figure 7: Pressure drop of air during the operation cycle of the TES tank

The dependence of the pressure drop value on the degree of heating of the rock material was proven during the study of the heat storage operation cycle. The difference between the values obtained for the cold tank and the hot tank was about 70 Pa. Figure 8 shows the temperature difference between the rock material and the air during the charging and discharging phases of the heat storage tank.
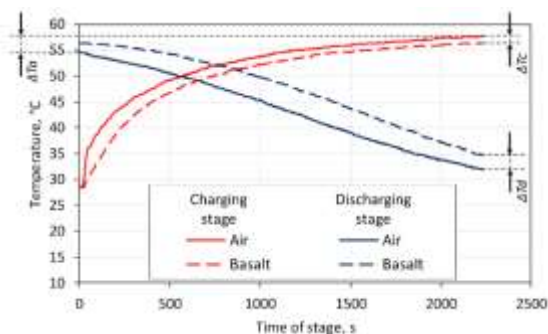
Figure 8: Difference between packed-bed material and air during the operation cycle of TES tank

In Figure 8, three temperature differences representing the exergy loss of the heat storage process in a basalt-packed bed are defined. During the charging phase, the temperature difference ΔT_c between the air charging the storage tank and the maximum temperature of the rock material at point T11 was recorded, which is due to imperfections in the heat transfer process. This value throughout the phase is not constant, with a final value of about 1.2°C. From the perspective of A-CAES operation, it is essential to maintain a high parameter of air directed to the expander. The temperature difference between the maximum temperature of the charge air and the return air is represented as ΔT_a. In a large-scale system, it is necessary to keep the difference between these values low to maintain the high exergy efficiency of the process. For the process under consideration, the difference between the maximum charging and return air temperatures was approximately 3°C. There was also a ΔT_d temperature difference during the discharge phase, which represents the difference between the maximum temperature of the rock material and the return air temperature. The average value of this parameter was approximately 1.22°C over the entire discharge phase, with a maximum value of 2°C. Using Equations (2-4), it was demonstrated that the exergy efficiency of the heat storage charging and discharging process was equal to 52.3% considering the relative humidity of the circulating air. The energy cycle efficiency of the TES storage tank was equal to 96.6%, indicating a high rate of energy accumulation in the rock material despite the lack of thermal insulation of the storage tank.

Summary

The presented basalt-filled laboratory-scale Thermal Energy Storage tank provides a basis for obtaining experimental data on the process of heat charging, storage, and discharge. The evaluation of the performance of a heat storage tank cannot be based only on the quantitative aspect of energy recovery, but also on the quality of the energy received represented by the temperature and pressure parameter of the regenerated air. Calculations pointed out that for the measurement series studied, the energy efficiency was 96.6% and the exergy efficiency was only 52.3%, indicating a significant decrease in the quality of the stored heat. Further research will focus on the effect of heat storage slenderness on the efficiency of the heat storage process, which will directly affect both the value of the air pressure drop, but also the heat

conduction field in the rock material. Simultaneous numerical studies will simulate and evaluate the performance of the TES tank in a large-scale A-CAES energy storage system.

Acknowledgments

References

[1] A. A. Kebede, T. Kalogiannis, J. van Mierlo, and M. Berecibar, "A comprehensive review of stationary energy storage devices for large scale renewable energy sources grid integration," *Renewable and Sustainable Energy Reviews*, vol. 159, p. 112213, May 2022, doi: 10.1016/J.RSER.2022.112213.

[2] S. Griffiths, B. K. Sovacool, J. Kim, M. Bazilian, and J. M. Uratani, "Decarbonizing the oil refining industry: A systematic review of sociotechnical systems, technological innovations, and policy options," *Energy Research & Social Science*, vol. 89, p. 102542, Jul. 2022, doi: 10.1016/J.ERSS.2022.102542.

[3] J. Kotowicz, D. Węcel, and M. Jurczyk, "Analysis of component operation in power-to-gas-to-power installations," *Applied Energy*, vol. 216, pp. 45–59, Apr. 2018, doi: 10.1016/J.APENERGY.2018.02.050.

[4] W. Uchman, A. Skorek-Osikowska, M. Jurczyk, and D. Węcel, "The analysis of dynamic operation of power-to-SNG system with hydrogen generator powered with renewable energy, hydrogen storage and methanation unit," *Energy*, vol. 213, p. 118802, Dec. 2020, doi: 10.1016/J.ENERGY.2020.118802.

[5] Ł. Bartela, A. Skorek-Osikowska, S. Dykas, and B. Stanek, "Thermodynamic and economic assessment of compressed carbon dioxide energy storage systems using a post-mining underground infrastructure," *Energy Conversion and Management*, vol. 241, p. 114297, Aug. 2021, doi: 10.1016/J.ENCONMAN.2021.114297.

[6] Ł. Bartela, M. Lutyński, G. Smolnik, and S. Waniczek, "Underground Compressed Air Storage Installation. European Patent Application," 20000302.8

[7] M. Cascetta, G. Cau, P. Puddu, and F. Serra, "A comparison between CFD simulation and experimental investigation of a packed-bed thermal energy storage system," *Applied Thermal Engineering*, vol. 98, pp. 1263–1272, Apr. 2016, doi: 10.1016/J.APPLTHERMALENG.2016.01.019.

[8] C. Prieto and L. F. Cabeza, "Thermal energy storage (TES) with phase change materials (PCM) in solar power plants (CSP). Concept and plant performance," *Applied Energy*, vol. 254, p. 113646, Nov. 2019, doi: 10.1016/J.APENERGY.2019.113646.

[9] N. Courtois, M. Najafiyazdi, R. Lotfalian, R. Boudreault, and M. Picard, "Analytical expression for the evaluation of multi-stage adiabatic-compressed air energy storage (A-CAES) systems cycle efficiency," *Applied Energy*, vol. 288, p. 116592, Apr. 2021, doi: 10.1016/J.APENERGY.2021.116592.

[10] H. Agalit, N. Zari, M. Maalmi, and M. Maaroufi, "Numerical investigations of high temperature packed bed TES systems used in hybrid solar tower power plants," *Solar Energy*, vol. 122, pp. 603–616, Dec. 2015, doi: 10.1016/J.SOLENER.2015.09.032.

[11] Y. Zhu, D. Wang, P. Li, Y. Yuan, and H. Tan, "Optimization of exergy efficiency of a cascaded packed bed containing variable diameter particles," *Applied Thermal Engineering*, vol. 188, p. 116680, Apr. 2021, doi: 10.1016/J.APPLTHERMALENG.2021.116680.

[12] W. Sebastian *et al.*, "Design and Construction Challenges for a Hybrid Air and Thermal Energy Storage System Built in the Post-Mining Shaft," *Journal of Thermal Science*, vol. 31, no. *, p. 2022, 2022, doi: 10.1007/s11630-022-1593-x.

[13] M. L. Jurczyk, S. Rulik, and L. Bartela, "Thermal energy storage in rock bed-CFD analysis," 2020.

[14] J. Ochmann, K. Rusin, S. Rulik, and Ł. Bartela, "Współczesne Problemy Ochrony Środowiska i Energetyki 2021 Identyfikacja współczynnika wnikania ciepła w procesie ładowania zasobnika Thermal Energy Storage na potrzeby adiabatycznego systemu CAES."

[15] S. M. White and C. L. Tien, "Analysis of flow channeling near the wall in packed beds*," 1987.

[16] N. Soares, C. Martins, M. Gonçalves, P. Santos, L. S. da Silva, and J. J. Costa, "Laboratory and in-situ non-destructive methods to evaluate the thermal transmittance and behavior of walls, windows, and construction elements with innovative materials: A review," *Energy and Buildings*, vol. 182, pp. 88–110, Jan. 2019, doi: 10.1016/J.ENBUILD.2018.10.021.

[17] M. Thebault, S. Giroux-Julien, V. Timchenko, C. Ménézo, and J. Reizes, "Transitional natural convection flow in a vertical channel: Impact of the external thermal stratification," *International Journal of Heat and Mass Transfer*, vol. 151, p. 119476, Apr. 2020, doi: 10.1016/J.IJHEATMASSTRANSFER.2020.119476.

[18] I. H. Bell, J. Wronski, S. Quoilin, and V. Lemort, "Pure and pseudo-pure fluid thermophysical property evaluation and the open-source thermophysical property library coolprop," *Industrial and Engineering Chemistry Research*, vol. 53, no. 6, pp. 2498–2508, Feb. 2014, doi: 10.1021/ie4033999.

[19] B. Rezaie, B. v. Reddy, and M. A. Rosen, "Exergy analysis of thermal energy storage in a district energy application," *Renewable Energy*, vol. 74, pp. 848–854, Feb. 2015, doi: 10.1016/J.RENENE.2014.09.014.

[20] L. Amiri, S. A. Ghoreishi-Madiseh, F. P. Hassani, and A. P. Sasmito, "Estimating pressure drop and Ergun/Forchheimer parameters of flow through packed bed of spheres with large particle diameters," *Powder Technology*, vol. 356, pp. 310–324, Nov. 2019, doi: 10.1016/J.POWTEC.2019.08.029.